ELSEVIER

Thermochimica Acta 258 (1995) 145–159

thermochimica acta

# Kinetic analysis of thermoanalytical data by extrapolating to infinite temperature

Nobuyoshi Koga

*Chemistry Laboratory, Faculty of School Education, Hiroshima University, 3-1-33 Shinonome, Minami-Ku, Hiroshima, 734, Japan*

Received 21 September 1994; accepted 22 December 1994

**Abstract**

The extrapolation of a set of thermoanalytical (TA) curves to infinite temperature is proposed as a possible method to calculate the kinetic parameters of solid-state reactions from the TA curves without assuming a constant heating rate. It is shown theoretically that the method is applicable for the TA curves under any temperature program if the kinetic model function does not change among the temperature conditions applied. The practical applicability of the method is investigated through the kinetic analysis of TA curves for the thermal decomposition of synthetic malachite $CuCO_3 \cdot Cu(OH)_2$. The present method of kinetic analysis is widely useful for nonlinear nonisothermal TA curves in which the sample temperature does not change linearly.

*Keywords:* Infinite temperature; Kinetics; Nonlinear nonisothermal TA; Solid-state reaction

## 1. Introduction

In conventional thermoanalytical (TA) methods, the heating rate of the sample or reference material is controlled to be constant by programming. Accordingly, kinetic analysis of conventional TA curves has been carried out by assuming a constant rate of variation of the sample temperature [1]. In practice, however, the assumption of a constant heating rate for the sample is not justified, owing to the effect of self-cooling or self-heating during reaction [2]. If the temperature in simultaneous TG–DTA measurements of the thermal decomposition of a solid is controlled by the measured temperature of the reference material, the linearly increasing temperature program is distorted by the effect of self-cooling during the reaction in accordance with the shape of the derivative DTA (DDTA) curve [3]. Although such deviation seems to be


*SSDI* 0040-6031(95)02249-X

improved somewhat by using heat compensation DSC or TA measurements in which the temperature is controlled by the measured sample temperature [4], the degree of improvement depends on the character of the reaction and the experimental conditions. In such TA measurements, the reaction under investigation takes place essentially under nonlinear nonisothermal conditions. For TA curves under the nonlinear nonisothermal conditions, temperature integration during the course of reaction, which is necessary for analyzing nonisothermal TA data kinetically [5], cannot be performed assuming a constant heating rate. This may be one of the most serious problems in kinetic approaches to thermal analysis.

On the other hand, the thermophysical properties of solids under nonlinear nonisothermal heating or cooling conditions are of interest as a new aspect of the TA approach, as can be seen from the TA techniques developed recently, e.g., controlled transformation rate thermal analysis (CRTA) [6], modulated DSC (MDSC) or dynamic DSC (DDSC) [7], high resolution TG (HRTG) [8] and so on. Methods of kinetic analysis for the TA curves under such nonlinear nonisothermal conditions are required for obtaining reliable kinetic parameters and for extending the usefulness of kinetic studies.

In the present paper, the extrapolation of a set of TA curves to infinite temperature is introduced as a possible method of kinetic analysis for nonlinear nonisothermal TA curves. A practical example of kinetic analysis is described for the thermal decomposition of synthetic malachite $CuCO_3 \cdot Cu(OH)_2$.

## 2. Theoretical

### 2.1. Temperature dependence of the reaction rate

For the kinetic analysis of TA curves of solid-state reactions, the following formula has widely been applied [1]

$$\frac{d\alpha}{dt} = A \exp\left(-\frac{E}{RT}\right) f(\alpha) \tag{1}$$

where $\alpha$, $A$, $E$, $R$ and $T$ are the fractional reaction, apparent pre-exponential factor, apparent activation energy, gas constant and temperature, respectively. The kinetic model functions $f(\alpha)$ are usually derived on the basis of the physico-geometric features of the reaction proceeding in a particle of the sample matrix [9]. Table 1 lists various $f(\alpha)$ usually employed for describing solid state reactions. Taking logarithms of Eq. (1), we obtain

$$\ln\left(\frac{d\alpha}{dt}\right) = -\frac{E}{RT} + \ln[A f(\alpha)] \tag{2}$$

Thus the plot of $\ln(d\alpha/dt)$ against the reciprocal temperature $T^{-1}$ at a given $\alpha$ under different heating rates $\phi$ represents a straight line with a slope of $-E/R$ unless the kinetic obedience to $f(\alpha)$ changes among the heating rates applied. The method for

Table 1
Theoretical kinetic model functions $f(\alpha)$ usually employed for the kinetic analysis of the solid-state reactions

| Model | Symbol | $f(\alpha)$ |
|---|---|---|
| Nucleation and growth | $A_m (m = 1, 1.5, 2, 2.5, 3, 4)$ | $m(1-\alpha)[-\ln(1-\alpha)]^{1-1/m}$ |
| Phase Boundary controlled Reaction | $R_n (n = 1, 2, 3)$ | $n(1-\alpha)^{1-1/n}$ |
| One-dimensional diffusion | $D_1$ | $1/2\alpha$ |
| Two-dimensional diffusion | $D_2$ | $-(1/\ln(1-\alpha))$ |
| Three-dimensional diffusion (Jander) | $D_3$ | $3(1-\alpha)^{2/3}/(2[1-(1-\alpha)^{1/3}])$ |
| Three-dimensional diffusion (Ginstling-Brounshtein) | $D_4$ | $3/(2[(1-\alpha)^{-1/3}-1])$ |

calculation of the apparent activation energy $E$ was originally proposed by Friedman [10] for chemical processes under linearly increasing temperatures.

The extended interpretation of the Friedman method was discussed by Ozawa [11], and the applicability of Eq. (2) to the processes of crystal growth from pre-existing nuclei and diffusion was shown mathematically. One of the most important findings of the extended interpretation of the Friedman method is that Eq. (2) can be applied to any TA data obtained isothermally and under any temperature changes. Because Eq. (2) is not limited by an assumption of constant heating rate, the Friedman method is applicable to TA curves in which the programmed temperature conditions have been distorted by self-cooling and/or self-heating effects, and also to CRTA curves. Such applicability was confirmed practically for the thermal dehydration processes of $Li_2SO_4 \cdot H_2O$ under a self-generated temperature condition [12].

The constancy of the apparent activation energy determined at different values of $\alpha$ is the necessary condition for further kinetic characterization based on the general kinetic equation Eq. (1), which in turn will be one of the criteria for examining the applicability of Eq. (1) to the reaction process under investigation [13].

### 2.2. *Generalized kinetic equation at infinite temperature*

Another finding of the Friedman method described above is the extrapolation of the rate data to infinite temperature. It is easily recognized that the intercepts of the Friedman plots represent the logarithmic reaction rate at infinite temperature. The kinetic rate equations at infinite temperature were successfully formalized by Ozawa more than 20 years ago by introducing the generalized time $\theta$ [14–16]

$$\theta = \int_0^t \exp\left(-\frac{E}{RT}\right) dt \tag{3}$$

Here, $\theta$ denotes the reaction time taken to attain a particular $\alpha$ at infinite temperature. First differentiation of Eq. (3) gives [15,16]

$$\frac{d\theta}{dt} = \exp\left(-\frac{E}{RT}\right) \tag{4}$$

Combining Eq. (4) with Eq. (1), we obtain [15,16]

$$\frac{d\alpha}{d\theta} = A f(\alpha) \tag{5}$$

Eq. (5) corresponds to the generalized kinetic equation at infinite temperature [17]. Using the pre-determined constant $E$ value, the reaction rate at infinite temperature $d\alpha/d\theta$ at the corresponding $\alpha$ is calculated from a set of experimental TA curves by the equation [16]

$$\frac{d\alpha}{d\theta} = \frac{d\alpha}{dt} \exp\left(\frac{E}{RT}\right) \tag{6}$$

Using Eq. (6), a plot of $d\alpha/d\theta$ against $\alpha$ is obtained as the kinetic rate data at infinite temperature.

Integration of Eq. (5) after rearrangement gives [14,16]

$$g(\alpha) = \int_0^\alpha \frac{d\alpha}{f(\alpha)} = A \int_0^\theta d\theta = A\theta \tag{7}$$

The integral kinetic equation at infinite temperature has the same form with that derived with the assumption of a constant heating rate [18].

### 2.3. Dependence of the rate data on the kinetic model function

A simple relationship between $d\alpha/d\theta$ and $f(\alpha)$ is deduced from Eq. (5), in which a plot of $d\alpha/d\theta$ against $f(\alpha)$ represents a straight line with slope $A$ when the correct $f(\alpha)$ has been employed. In such an approach, however, the value of $A$ is distorted from the true value, as a simple mathematical consequence [19], if the actual kinetic process cannot be fully described by the conventional $f(\alpha)$. In this respect, it can be useful to find an empirical function $h(\alpha)$ containing the smallest possible number of kinetic exponents instead of $f(\alpha)$, so that there is enough flexibility to describe the real process as closely as possible. One such empirical functions is known as the Sestak–Berggren model [20]

$$h(\alpha) = \alpha^m (1-\alpha)^n [-\ln(1-\alpha)]^p \tag{8}$$

It was believed that this kinetic equation, containing as many as three kinetic exponents, would be able to describe any TA curve. However, empirical kinetic models containing more than two kinetic exponents are too complicated to evaluate the kinetic exponents in practice [21, 22]. The empirical kinetic model functions $h(\alpha)$ employed in the present work are listed in Table 2. If the most appropriate $h(\alpha)$ has been determined, the apparent values of $A$ at different $\alpha$ are calculated according to Eq. (5). Using the appropriate $h(\alpha)$, a constant value of $A$ is obtained at different $\alpha$, which is used as one of the criteria for the appropriate kinetic treatment [23]. Knowing the most appropriate $h(\alpha)$ and constant $A$, integration of the general kinetic equation at infinite temperature is performed to obtain the integral kinetic rate data expressed by Eq. (7).

However, the physico-geometric feature of the process as assumed in the formulation of $f(\alpha)$ is difficult to predict from the $h(\alpha)$ determined, because of the essentially

Table 2
Empirical kinetic model functions $h(\alpha)$, together with their integral forms $g(\alpha)$

| Type | Symbol | $h(\alpha)$ | $g(\alpha) = \int_0^\alpha (d\alpha/h(\alpha))$ |
|---|---|---|---|
| Johnson–Mehl–Avrami–Erofeyev | JMA($M$) | $M(1-\alpha)[-\ln(1-\alpha)]^{1-1/M}$ | $[-\ln(1-\alpha)]^{1/M}$ |
| Reaction order | RO($N$) | $(1-\alpha)^N$ | $(1-(1-\alpha)^{1-N})/(1-N)$ |
| Diffusion based | DF($N$) ($N>2$) | $1/[(1-\alpha)^{2/N}-1]$ | $(N/2)-\alpha-(N/2)(1-\alpha)^{2/N}$ |
| Sestak–Berggren | SB($M$, $N$) | $\alpha^M(1-\alpha)^N$ | no analytical form |

empirical character of $h(\alpha)$. It is interesting here to introduce the semi-empirical kinetic model functions $h(\alpha)$ [24]. Introducing the accommodation function $a(\alpha)$ [25], the semi-empirical model function $h(\alpha)$ is expressed as

$$h(\alpha) = f(\alpha)a(\alpha) \tag{9}$$

Then the kinetic expression $h(\alpha)$ can be regarded as a distorted case of the theoretical $f(\alpha)$, with a possible $a(\alpha)$ to decrease the difference of the idealized $f(\alpha)$ from the practical process. Application of the fractal dimension to the $f(\alpha)$ is one of the simplest examples of such semi-empirical $h(\alpha)$ [26]. Table 3 lists the semi-empirical $h(\alpha)$ functions, together with their mathematical properties.

Multiplication of the function $h(\alpha)$ with the integral function $g(\alpha)$ is a useful diagnostic tool to estimate the applicability of the semi-empirical $h(\alpha)$ as well as the shape of $h(\alpha)$ and the value of $\alpha$ at the maximum of $h(\alpha)$, i.e., $\alpha_M$, because the respective functions $h(\alpha)g(\alpha)$ represent the maximum at the characteristic value of $\alpha$, i.e., $\alpha_p$ [27]. The values of $\alpha_M$ and $\alpha_p$ are also listed in Table 3. From Eqs. (5) and (7), we obtain

$$h(\alpha)g(\alpha) = \frac{d\alpha}{d\theta}\theta \tag{10}$$

Using the empirical $h(\alpha)$ determined above, the experimental value of $\alpha_p$ is obtained from Eq. (10). The semi-empirical $h(\alpha)$ suitable for describing the kinetic rate data can be distinguished by the correspondence of the shape of $h(\alpha)$ and the values of $\alpha_M$ and $\alpha_p$ [13,27,28]. The most appropriate kinetic exponent in the semi-empirical $h(\alpha)$ is determined through the plots according to Eq. (5) and/or Eq. (7) by continuously changing the kinetic exponent [29]. Although the semi-empirical $h(\alpha)$ could not show better correspondence to the experimental data than the empirical $h(\alpha)$, it is hoped that the physico-geometric feature expected from the semi-empirical $h(\alpha)$ will give useful information for further investigations complemented by other physico-chemical measurements, e.g., microscopy techniques [17,18,30–32].

## 3. Experimental

Synthetic malachite was prepared by the titration of 1 M $CuSO_4$ solution with 1 M $K_2CO_3$ solution [33]. With mechanical stirring, the precipitate produced during

Table 3
The semi-empirical kinetic model functions $h(\alpha) = f(\alpha)a(\alpha)$, together with their mathematical properties

| Symbol | Range of exponent | $h(\alpha)$ | Shape of $h(\alpha)$ | $\alpha_M$ [a] | $g(\alpha) = \int_0^\alpha (d\alpha/h(\alpha))$ | $\alpha_p$ [b] |
|---|---|---|---|---|---|---|
| $A_M$ | $1 \le M \le 4$ | $M(1-\alpha)[-\ln(1-\alpha)]^{1-1/M}$ | Peak | $0 \le \alpha_M \le 0.632$ | $[-\ln(1-\alpha)]^{1/M}$ | 0.632 |
| $R_N$ | $1 \le N \le 3$ | $N(1-\alpha)^{1-1/N}$ | Convex | 0 | $1-(1-\alpha)^{1/N}$ | $0.704 \le \alpha_p \le 1.0$ |
| $D_N$ | $1 \le N < 2$ | $1/[1-(1-\alpha)^{2/N-1}]$ | Concave | 0 | $-(N/2)+\alpha+(N/2)(1-\alpha)^{2/N}$ | $0.834 < \alpha_p \le 1.0$ |
| | $N = 2$ | $-(1/\ln(1-\alpha))$ | Concave | 0 | $\alpha+(1-\alpha)\ln(1-\alpha)$ | 0.834 |
| | $2 < N \le 3$ | $1/[(1-\alpha)^{2/N-1}-1]$ | Concave | 0 | $(N/2)-\alpha-(N/2)(1-\alpha)^{2/N}$ | $0.774 \le \alpha_p < 0.834$ |

[a] Value of $\alpha$ at the maximum of $h(\alpha)$.
[b] Value of $\alpha$ at the maximum of $h(\alpha)g(\alpha)$.

the titration was aged in the mother liquor at 50°C for 2 h. The precipitate was filtered off, washed with water and ethanol, and dried in air at 100°C. The product was identified by chemical analysis for $Cu^{2+}$, FT-IR spectroscopy, X-ray powder diffractometry and TG.

A 10.0 mg amount of the sample was weighed into a platinum crucible 2.5 mm in diameter and 5 mm in height. Simultaneous TG–DTA curves at various programmed heating rates were recorded using an ULVAC TGD-9400 instrument with an IR image furnace, in which the temperature was controlled by the measured sample temperature. The atmospheric pressure during the measurement was controlled to be $1.5 \times 10^{-2}$ Pa using a vacuum controller. The TA data were calibrated by the data from blank measurements. Fig. 1 shows a typical experimental heating rate around the decomposition temperature in the present TG–DTA measurements. A positive deviation of the practical heating rate from the programmed value is seen at the initial stage of the reaction, which may be caused by overshooting from the furnace to recover the endothermic reaction. Accordingly, for the present TA curves it is difficult to assume a constant heating rate during the reaction.

## 4. Results and discussion

Fig. 2 shows typical TG–DTG curves for the thermal decomposition of synthetic malachite at different applied heating rates. In these TA measurements, the practical

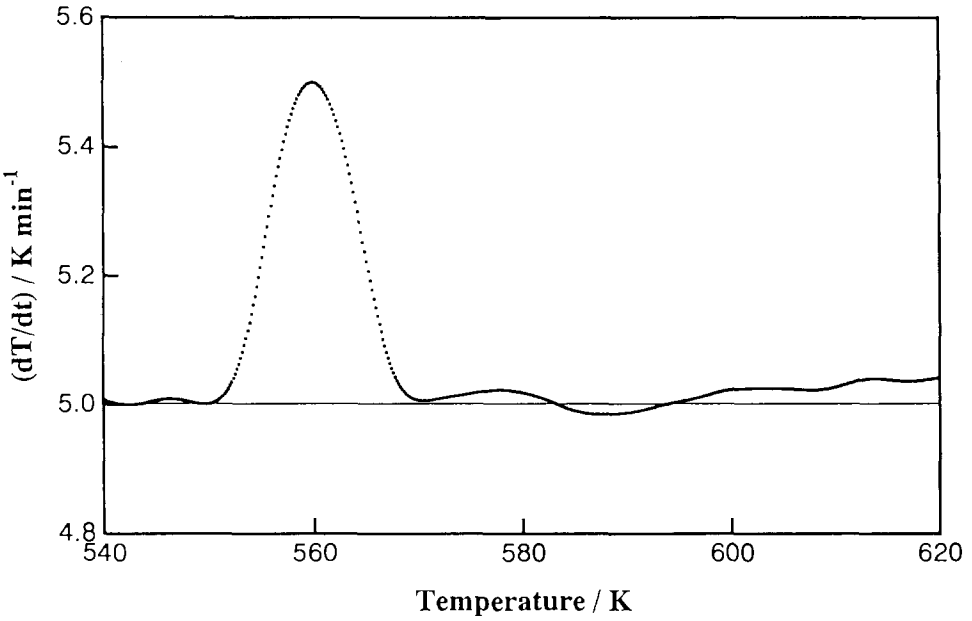


Fig. 1. A typical plot of the practical heating rate $dT/dt$ against temperature $T$ in the present TG–DTA measurements at a programmed heating rate of 5 K $min^{-1}$.

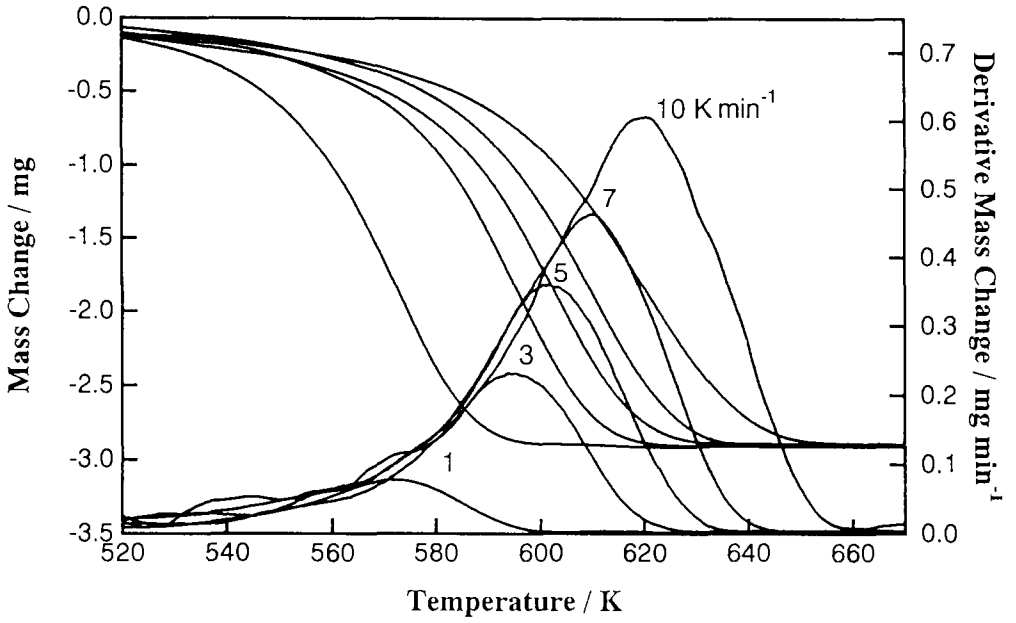


Fig. 2. Typical TG–DTG curves for the thermal decomposition of synthetic malachite under a reduced pressure of $1.5 \times 10^{-2}$ Pa at various programmed heating rates.

heating rate during the reaction was distorted irrespective of the heating rate applied, typically as shown in Fig. 1. The Friedman plots at various $\alpha$ are shown in Fig. 3. The respective plots represent good linearity, with the correlation coefficient of the linear regression analysis $\gamma$ better than $-0.9900$. Fig. 4 shows the $\alpha$ dependence of the apparent value of $E$. A nearly constant $E$ value was obtained in the range $0.2 \leq \alpha \leq 0.95$ with a mean value of $131.3 \pm 0.4$ kJ mol$^{-1}$. The constancy of the $E$ value at different $\alpha$ is a prerequisite of the application of the general kinetic equation, i.e., Eq. (1). The results in Fig. 4 indicate that the present reaction can be treated on the basis of Eq. (1) within the restricted range of $0.2 \leq \alpha \leq 0.95$.

The kinetic rate data extrapolated to infinite temperature were obtained by applying the mean value of $E$ to Eq. (6) within the restricted range $0.2 \leq \alpha \leq 0.95$. Fig. 5 represents such kinetic rate data at infinite temperature as a plot of $d\alpha/d\theta$ against $\alpha$. According to Eq. (5), the obedience of the rate data to the theoretical kinetic model function was compared through the plots of various $f(\alpha)$, listed in Table 1, against $d\alpha/d\theta$. Any plot of $f(\alpha)$ against $d\alpha/d\theta$ did not show a linear relationship, as is seen from Fig. 6.

To avoid deviation of the apparent $A$ value due to the inappropriate kinetic model function, the empirical kinetic model functions $h(\alpha)$ listed in Table 2 were employed. Because the reaction rate at infinite temperature $d\alpha/d\theta$ reaches its maximum at $\alpha_M = 0.37$, see Fig. 5, the rate data are probably described by the SB($M$,$N$) or JMA($M$) model [13, 22, 27, 28]. The kinetic exponents $M$ and $N$ in the SB($M$,$N$) function are

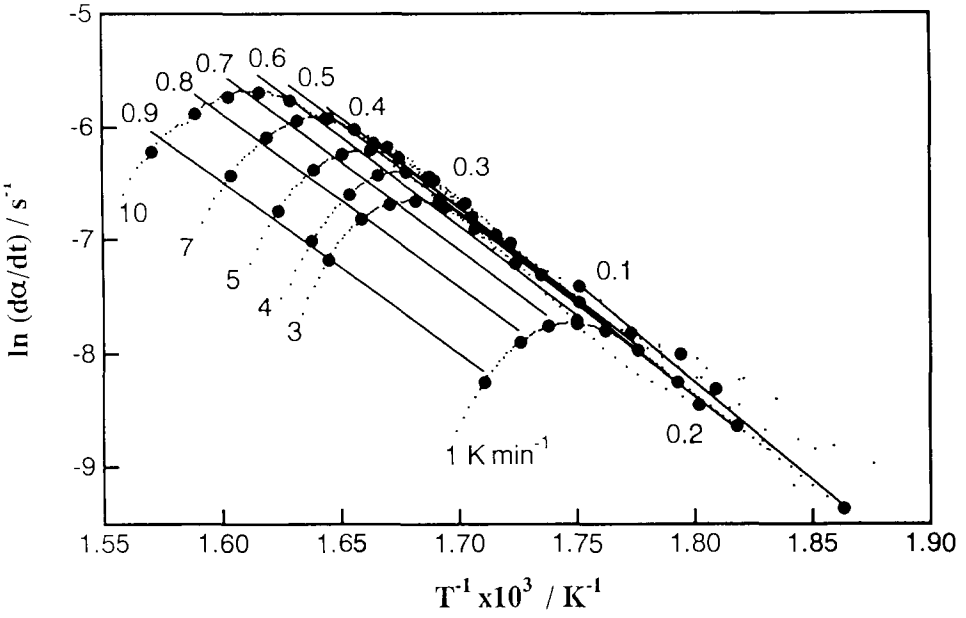


Fig. 3. Typical plots of $\ln(d\alpha/dt)$ against $T^{-1}$ at various values of $\alpha$ from 0.1 to 0.9 in steps of 0.1.

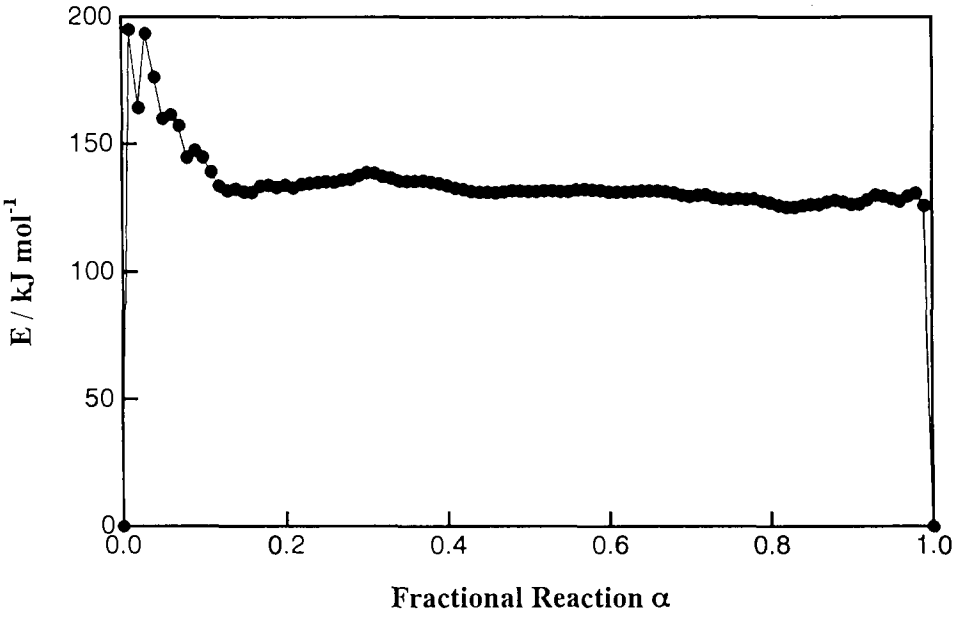


Fig. 4. The values of $E$ at various $\alpha$ calculated by the Friedman method.

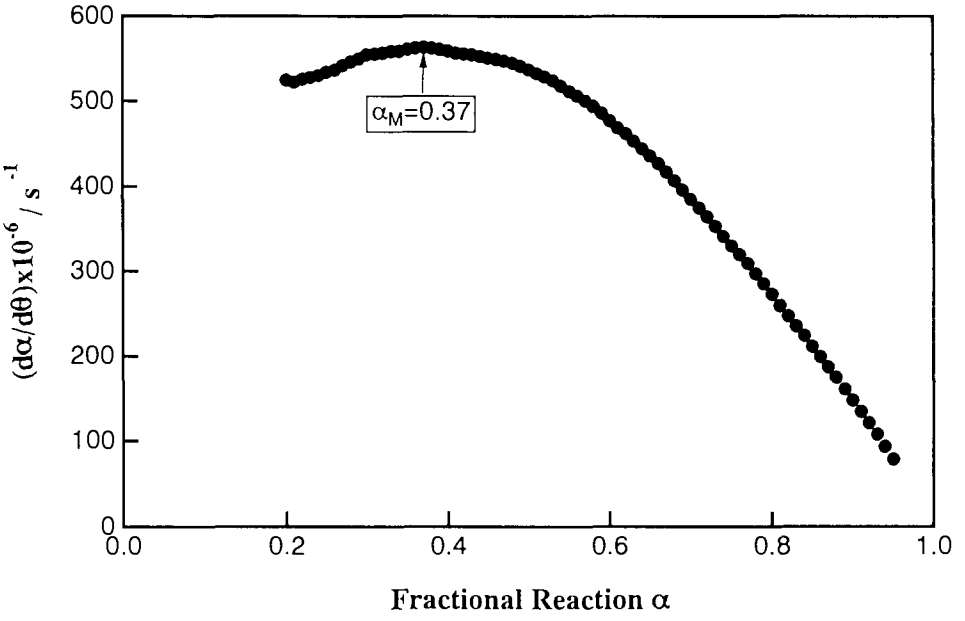


Fig. 5. The plot of $d\alpha/d\theta$ againt $\alpha$ in the restricted range $0.2 \leq \alpha \leq 0.95$.

estimated using the following relationship

$$\ln\left(\frac{d\alpha}{d\theta}\right) = \ln A + N \ln[\alpha^P(1-\alpha)] \tag{11}$$

with

$$P = \frac{M}{N} = \frac{\alpha_M}{1-\alpha_M}$$

Fig. 7 shows the plot of $\ln(d\alpha/d\theta)$ against $\ln[\alpha^P(1-\alpha)]$ with $P=0.587$. The plot represents fairly good linearity with $\gamma = 0.9996$, from which the exponents $N = 1.01$ and $M = NP = 0.60$ are determined. For the JMA($M$) model, the exponent $M$ was determined using the equation [13, 22, 27, 28].

$$M = \frac{1}{1 + \ln(1-\alpha_M)} \tag{12}$$

The value of $M$ in the JMA($M$) function calculated from Eq. (12) was 1.86. Fig. 8 shows the plots of two possible $h(\alpha)$, SB(0.60,1.01) and JMA(1.86), against $d\alpha/d\theta$ according to Eq. (5). It is seen from Fig. 8 that the SB(0.60,1.01) function describes well the shape of the kinetic rate data with $\gamma = 0.9994$. The apparent values of $A$ at different $\alpha$ calculated using Eq. (5) are shown in Fig. 9. The nearly constant value of $\ln A = 21.21 \pm 0.02\,s^{-1}$ was obtained for the SB(0.60,1.01) model. The values obtained for the JMA(1.86) model

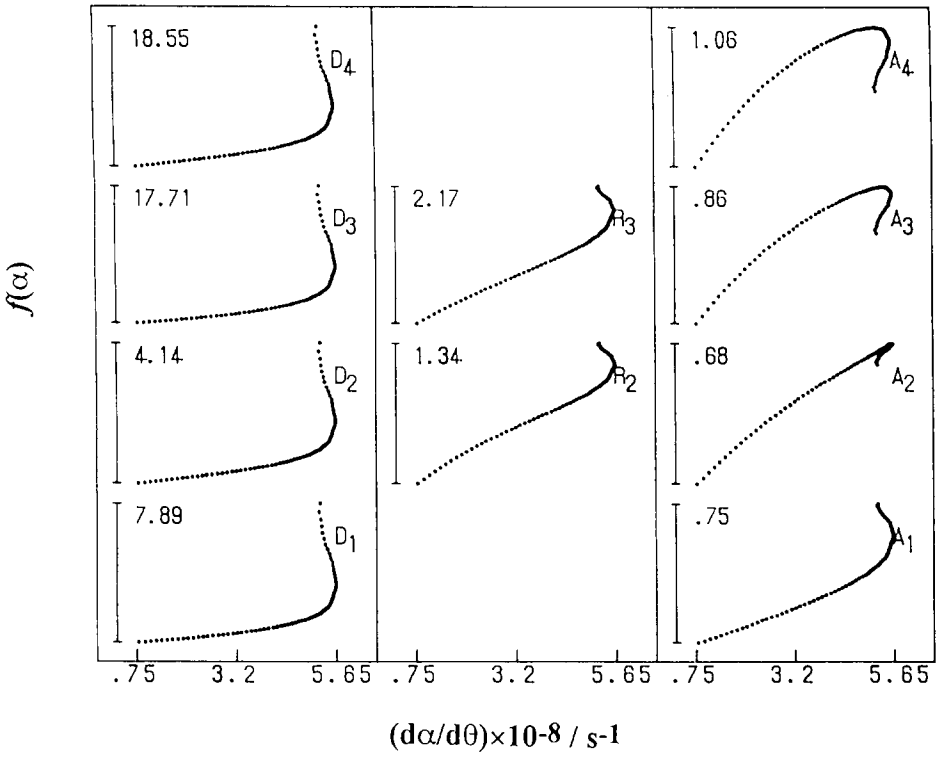


Fig. 6. Plots of various $f(\alpha)$ against $d\alpha/d\theta$ in the restricted range $0.2 \leq \alpha \leq 0.95$.

decrease gradually with $\alpha$. The constancy of the apparent values of $A$ irrespective of $\alpha$ is also a prerequisite of Eq. (1), in addition to a constant value of $E$. This is in turn one of the criteria to evaluate whether or not the appropriate kinetic treatments were performed [23]. Accordingly, the SB(0.60,1.01) model can be selected as the most appropriate empirical kinetic model function. Fig. 10 shows the correspondence of the experimental values of $d\alpha/Ad\theta$ to the mathematically drawn SB(0.60,1.01) function. Within the restricted range of $0.2 \leq \alpha \leq 0.95$, the rate data correspond perfectly to the SB(0.60,1.01) function with the standard deviation of the nonlinear regression analysis $\sigma = 0.0003$.

A plot of $h(\alpha)g(\alpha)$ against $\alpha$ was drawn by numerically integrating the SB(0.60,1.01) function with respect to $0 \leq \alpha \leq 1$, as shown in Fig. 10. The function $h(\alpha)g(\alpha)$ reaches a maximum at $\alpha_p = 0.60$, which corresponds very closely with the specific value of $\alpha_p = 0.632$ for the semi-empirical $A_M$ model listed in Table 3. The most appropriate kinetic exponent $M = 1.80$ in the $A_M$ model was determined from the linearity of the $d\alpha/d\theta$ vs. $A_M$ plots by changing the value of $M$ from 1.00 to 4.00 in steps of 0.01. Fig. 11 shows the plot of $d\alpha/d\theta$ against $A_{1.80}$. The apparent values of $A$ at different $\alpha$ obtained by assuming the semi-empirical $A_{1.80}$ model are also shown in Fig. 9. The constancy of

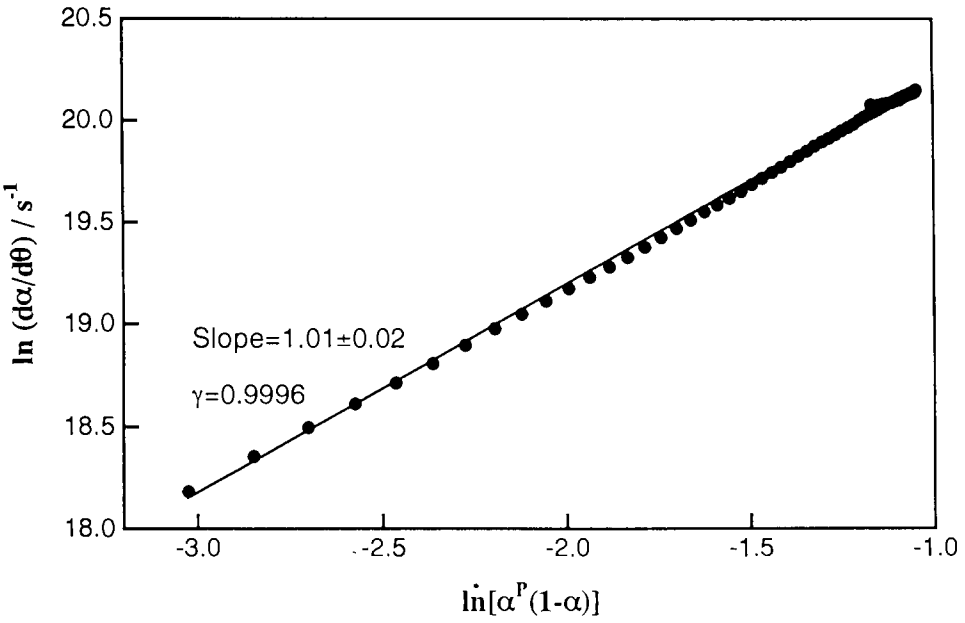


Fig. 7. The plot of $\ln(d\alpha/d\theta)$ against $\ln[\alpha^P(1-\alpha)]$ with $P = 0.587$ in the restricted range $0.2 \leq \alpha \leq 0.95$.

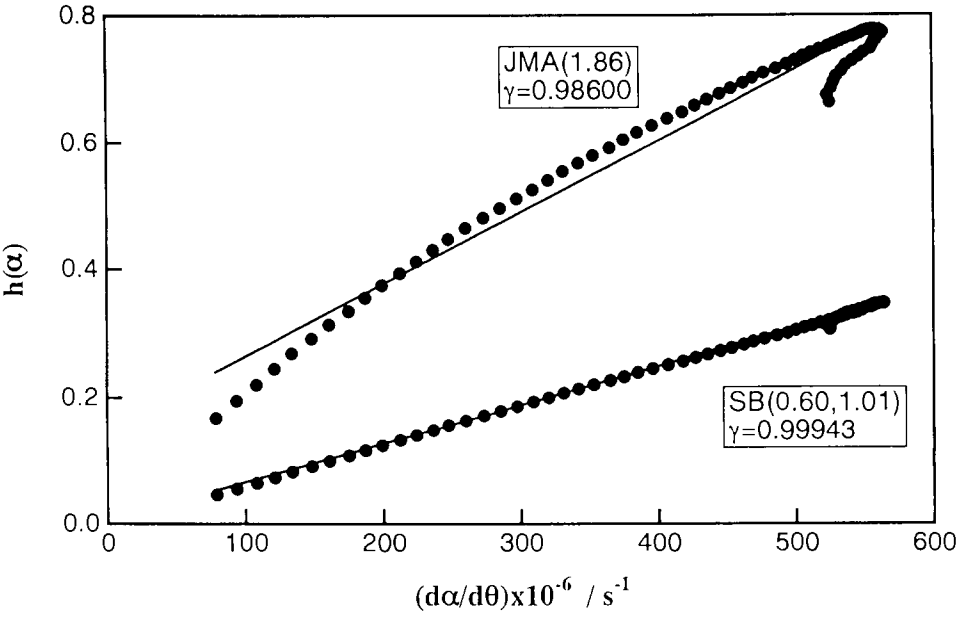


Fig. 8. Plots of the two possible $h(\alpha)$; SB(0.60,1.01) and JMA(1.86) against $d\alpha/d\theta$ in the restricted range $0.2 \leq \alpha \leq 0.95$.

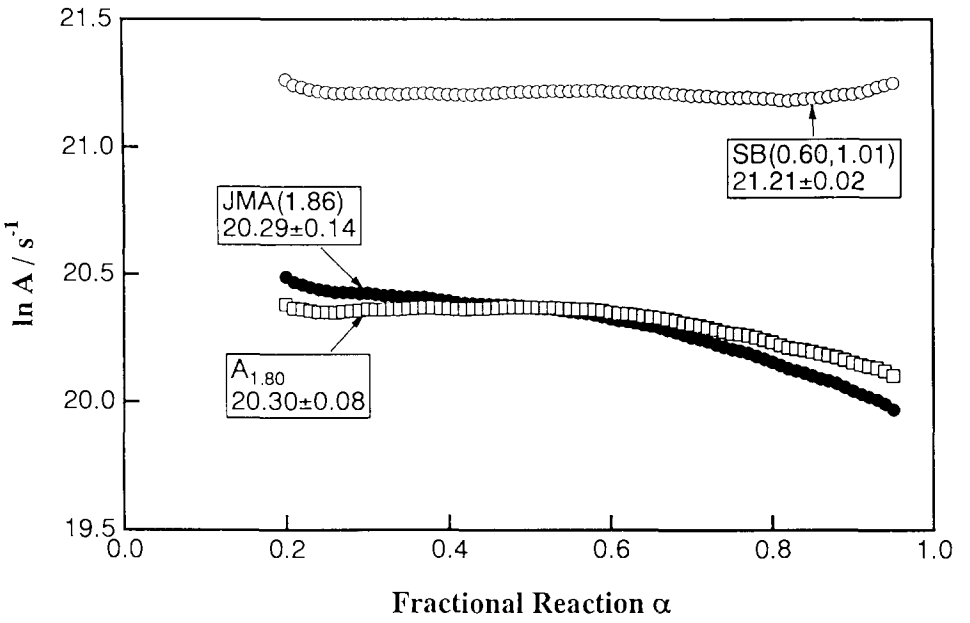


Fig. 9. The values of ln$A$ at various $\alpha$ calculated by Eq. (5) assuming the empirical SB(0.60,1.01) and JMA(1.86) functions and the semi-empirical $A_{1.80}$ function in the restricted range $0.2 \leq \alpha \leq 0.95$.

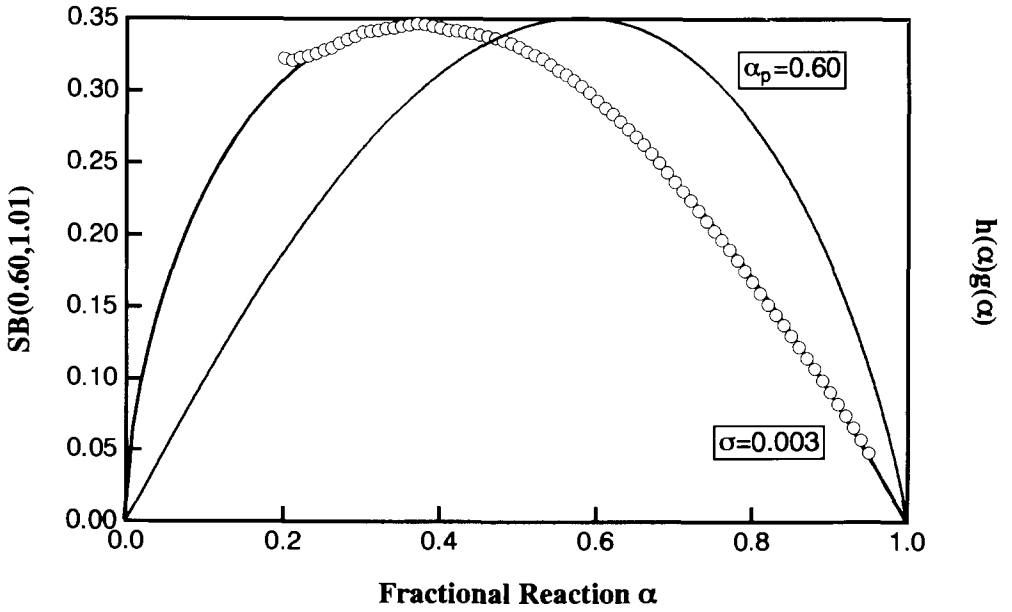


Fig. 10. Plots of $h(\alpha)$ and $h(\alpha)g(\alpha)$ against $\alpha$ according to the empirical SB(0.60,1.01) function, together with the plot of experimental $d\alpha/Ad\theta$ (O) against $\alpha$ in the restricted range $0.2 \leq \alpha \leq 0.95$.

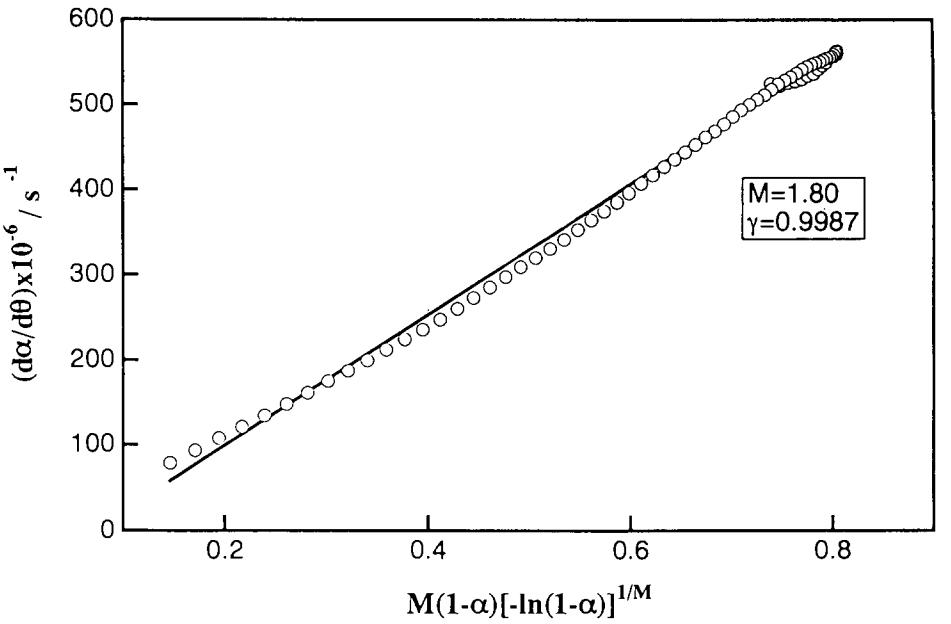


Fig. 11. The plot of $d\alpha/d\theta$ against the semi-empirical $A_{1.80}$ function in the restricted range $0.2 \leq \alpha \leq 0.95$.

$\ln A$ is slightly improved from the JMA(1.86) model. The difference of the absolute values of $\ln A$ for the $A_{1.80}$ and SB(0.60,1.01) models arises from the meaning of the apparent rate constant assumed in formulating these model functions. The semi-empirical $A_{1.80}$ model can be interpreted on the basis of the theoretical $A_m$ model as is regulated by the nucleation of the product crystallites and their growth with the fractal dimension [24].

## 5. Conclusions

Without assuming a constant heating rate during the reaction, the temperature integration of the general kinetic equation becomes difficult, so that the kinetic equation in an integral form cannot be applied to the thermoanalytical data. An isoconversion method based on Eq. (1), known as the Friedman method, is useful for obtaining the apparent values of $E$ at different $\alpha$ for nonlinear nonisothermal TA curves because a constant heating rate is not assumed in the method. Using a constant value of $E$ during the reaction, the set of TA data is extrapolated to infinite temperature according to Eq. (6). The rate data at infinite temperature can be described by the general kinetic equation with the generalized time $\theta$, Eq. (5). If the correct kinetic model function is applied, the general kinetic equation at infinite temperature can be integrated with respect to $\theta$ without the assumption of a constant heating rate. The

empirical kinetic model functions $h(\alpha)$, such as the Sestak–Berggren model, play an important role in this integration, because of their flexibility in describing the kinetic rate data. Using both differential and integral kinetic equations at infinite temperature, the kinetic obedience to an appropriate kinetic model function has been evaluated thoroughly. Employing the semi-empirical kinetic model functions $h(\alpha)$, expressed by multiplying the theoretical kinetic model function $f(\alpha)$ with an accommodation function $a(\alpha)$, it is possible to interpret the physico-geometrical feature of the reaction. Through the kinetic analysis, the constancy of the values of $E$ and $A$, a prerequisite of the general kinetic equation, in turn provides the criterion for the appropriate kinetic analysis.

## References

[1] J. Sestak, Thermophysical Properties of Solids, Elsevier, Amsterdam, 1994.
[2] J. Sestak, Talanta, 13 (1966) 567; Silikaty, 7 (1963) 125.
[3] J.P. Czarnecki, N. Koga, V. Sestakova and J. Sestak, J. Therm. Anal., 38 (1992) 575.
[4] H. Tanaka and N. Koga, J. Therm. Anal., 36 (1990) 2601.
[5] J. Sestak, J. Therm. Anal., 16 (1979) 503.
[6] J. Rouquerol, J. Therm. Anal., 5 (1973) 203.
[7] M. Reading, TRIP, 1 (1993) 248.
[8] M. Reading, in E.L. Charsley and S.B. Warrington (Eds.), Thermal Analysis — Techniques & Applications, Royal Society of Chemistry, London, 1993, p. 126.
[9] M.E. Brown, D. Dollimore and A.K. Galwey, Reactions in the Solid State, Elsevier, Amsterdam, 1980.
[10] H.L. Friedman, J. Polym. Sci., Part C, C6 (1964) 183.
[11] T. Ozawa, J. Therm. Anal., 31 (1986) 547.
[12] N. Koga and H. Tanaka, Thermochim. Acta, 224 (1993) 141.
[13] N. Koga, J. Malek, J. Sestak and H. Tanaka, Netsu Sokutei, 20 (1993) 210.
[14] T. Ozawa, Bull. Chem. Soc. Jpn., 38 (1965) 1881.
[15] T. Ozawa, J. Therm. Anal., 2 (1970) 301.
[16] T. Ozawa, Thermochim. Acta, 100 (1986) 109.
[17] N. Koga and H. Tanaka, J. Phys. Chem., 98 (1994) 10521.
[18] N. Koga and H. Tanaka, J. Phys. Chem., 93 (1989) 7793.
[19] N. Koga, J. Sestak and J. Malek, Thermochim. Acta, 188 (1991) 333.
[20] J. Sestak and G. Berggren, Thermochim. Acta, 3 (1971) 1.
[21] V.M. Gorbatchev, J. Therm. Anal., 18 (1980) 194.
[22] J. Malek, Thermochim. Acta, 138 (1989) 337.
[23] N. Koga, Thermochim. Acta, 244 (1994) 1.
[24] N. Koga and H. Tanaka, J. Therm. Anal., 41 (1994) 455.
[25] J. Sestak, J. Therm. Anal., 36 (1990) 1997.
[26] R. Ozao and M. Ochiai, J. Ceram. Soc. Jpn., 101 (1993) 263.
[27] J. Malek, Thermochim. Acta, 200 (1992) 257.
[28] J. Sestak and J. Malek, Solid State Ionics, 63/65 (1993) 245.
[29] N. Koga, S. Takemoto, S. Okada and H. Tanaka, Thermochim. Acta, in press.
[30] A.K. Galwey, Thermochim. Acta, 96 (1985) 259; React. Solids, 8 (1990) 211.
[31] A.K. Galwey, N. Koga and H. Tanaka, J. Chem. Soc. Faraday Trans., 86 (1990) 531.
[32] H. Tanaka, N. Koga and A.K. Galwey, J. Chem. Educ., in press.
[33] H. Tanaka and M. Yamane, J. Therm. Anal., 38 (1992) 627.